53. PHYSICAL AND MECHANICAL PROPERTIES OF THE BLACK SEA'S PLIOCENE-QUATERNARY SEDIMENTS (Sites 380 and 381)

P. N. Kuprin, F. A. Stcherbakov, A. S. Poljakov, and V. G. Shlikov, Laboratory of Marine Geology, Geological Department of Moscow University, Moscow
and
M. P. Nesterova, A. J. Shevchenko, N. V. Turanskaja, and V. P. Kazakova, Analytical Laboratory of P. P. Shirshov Institute of Oceanology, Moscow

INTRODUCTION

The Pliocene-Quaternary deposits recovered by deep-sea drilling in the Black Sea make up a continuous section with a clearcut transition from unconsolidated sediment to rock. Distinction between them has never been clearly defined and can be expected only from studies on a great number of sections formed in various parts of the world oceans. Above all, they should be deposits resulting from continuous accumulation, free of any discontinuities; the Pliocene-Quaternary deposits of the Black Sea meet this requirement almost ideally.

Sediment is transformed into rock as a result of internal diagenesis under the influences of biochemical and geochemical processes, pressure, and temperature; original properties such as strength, consistency, volume weight, etc., become transformed. Study of such features, "the physical and mechanical properties," can yield much qualitative and quantitative information as to the direction and intensity of the post-depositional changes in each interval of the sedimentary series. This was the chief aim of the present research.

Our investigation of physical and chemical properties was conducted on material placed at our disposal by Leg 42B Scientist Co-Chief, V. P. Neprochnov (Table 1). Ten monolith samples, expressly taken at Site 381, by onboard research group member, E. S. Trimonis, were 10-cm core pieces uncut along the longitudinal axis, and treated with paraffin to preserve humidity and natural texture. In addition, 50 wet samples, with a disturbed texture, recovered from various depths of Holes 380/380A, were studied. Several of these samples, recovered from greater depths (approximately 200-300 m), were nearly intact, enabling a wider set of physical and mechanical properties to be investigated.

LITHOLOGICAL DESCRIPTION OF THE SECTION

A study of the mineralogical composition of both larger sediment particles 0.1-0.05 cm in size and clay particles smaller than 0.001 mm was made. The former were separated in a heavy liquid (Table 2) and then studied in an immersion liquid. Clay minerals were studied using an X-ray diffractometer with Cuα radiation at voltage Uα = 33 kv, current intensity Iα = 10 ma, and slit width 1; 0.5; 0.25 mm. The specimens were prepared from (a) oriented particles, (b) glycerine treated, and (c) heated to 500°C for one hour. X-ray diffraction patterns of these specimens are given in Figure 1 and Table 3. The percentage of each clay mineral was computed from the diffraction patterns after Weaver (1967).

The chemical composition of several samples typical of certain lithological types of deposits was studied as well. In particular, usual analysis techniques were applied to determine 10 elements represented by oxides and to estimate their content in weight percentages (Table 4). For some samples which did not contain enough material, only iron, manganese, and titanium were determined with these techniques. In some samples, also poor in material, elements were determined by X-ray fluorescence analysis.

For almost all samples, the $C_{org.}$ content and the CO_2 content were determined by the Knopp method. The results are given in Table 5. From the CO_2 content, $CaCO_3$ was later estimated in all samples.

A group of samples distributed across the whole section was subjected to an analysis of amorphous silica content, which was measured in soda extract (Table 6). Ca and Mg determinations were carried out for a number of reference samples in hot muriatic extract (HCl 2.5%). The results, in percentage of the deposit mass, are given in Table 7. Combined results are shown in Figure 2. The larger numbers in Figure 2 are arithmetic means of the content of a component in the pertinent interval. The deposits' contents in the figure are divided into four categories. The first of these characterizes size distribution, the second refers to the mineralogy of larger silt particles, the third describes the contents of the main clay minerals, and the fourth indicates certain important properties of the chemical composition.

Although our intervals largely coincide with those tentatively fixed by the onboard group, our data suggest a somewhat different assessment of the individual components' contributions. In particular, the upper part of the section (up to 300 m thick) appears to be a typical terrigenous series, perhaps more finely dispersed than originally reported. These sediments are classified as silt-clay. The wide range of size distribution suggests that they most likely accumulated in a deep-sea basin. The series as a whole resembles the Neo-Euxinian silts, occurring at the base of the continental slope of the South Crimea. The predominance of terrigenous clay matter here (primarily hydromica) masks the biogenic components, and the series as a whole cannot be referred to as diatomaceous ooze.

At 350 meters sub-bottom, deposits abruptly become enriched in carbonate; the series (from 350-650 m) can be described as carbonaceous clay.

TABLE 1
List of Samples Studied From Holes 380/380A and 381

Core	Section	Depth Below Sea Floor (m)	Condition of the Sample: Deformate	Condition of the Sample: Not Deformate
Hole 380				
0	CC	9.5	+	–
4	CC	38.0	+	–
5	CC	47.5	+	–
7	CC	66.5	+	–
9	CC	85.5	+	–
11	CC	104.5	+	–
13	CC	123.5	+	–
15	CC	142.5	+	–
17	CC	161.5	+	–
20	CC	190.0	+	–
22	CC	209.0	+	–
23	mop.	209.5	+	–
25	CC	237.5	+	–
27	CC	256.5	+	–
29	CC	275.5	+	–
33	CC	313.5	+	–
36	CC	342.0	+	–
38	CC	361.0	+	–
39	CC	370.5	+	–
Hole 380A				
5	CC	380.0	–	+
7	CC	399.0	+	–
8	CC	408.5	+	–
10	CC	427.5	+	–
12	CC	446.5	+	–
14	CC	465.5	–	+
16	CC	484.5	+	–
18	CC	503.5	+	–
20	CC	522.5	–	+
22	CC	541.5	+	–
26	CC	579.5	–	+
29	CC	598.5	+	–
33	CC	636.5	+	–
36	CC	665.0	–	+
40	CC	703.0	–	+
43	CC	731.5	+	–
45	mop.	741.0	–	+
48	CC	778.5	–	+
52	CC	817.0	–	+
56	CC	855.0	–	+
60	CC	893.0	+	–
66	CC	950.0	+	–
71	CC	997.5	–	+
Site 381				
7	CC	66.5	–	+
9	mop.	76.0	–	+
10	CC	95.0	–	+
13	CC	123.5	–	+
14	mop.	124.0	–	+
19	mop.	171.0	–	+
22	CC	199.5	–	+
26	CC	237.5	–	+
31	CC	285.0	–	+
33	CC	304.0	–	+

In deeper horizons the deposits differ in that diagenetic processes are more strongly pronounced, as expressed in a heightened pyritization and in irreversible aggregation of clay particles, which affects the granulometric composition. Zeolites, which we believe to be authigenic, support this contention. Further, below 700 meters, biogenic components

TABLE 2
Percentage Content of Heavy and Light Minerals in the 0.1-0.05 mm Fraction

Core	Weight of the Fraction 0.1-0.05	Weight of the Heavy Minerals	Weight of the Light Minerals	Percentage of the Heavy Minerals	Percentage of the Light Minerals
Hole 380					
0	0.6089	0.0042	0.6047	0.69	99.31
4	0.1835	0.0085	0.1749	4.69	95.31
5	0.7608	0.0337	0.7271	4.43	95.57
7	0.0254	0.0007	0.0247	2.76	97.24
9	0.0112	0.0009	0.0103	8.04	91.96
11	0.0375	0.0006	0.0369	1.60	98.40
15	1.3188	0.0255	1.2933	1.93	98.07
17	0.0338	0.0009	0.0329	2.66	97.34
20	0.0726	0.0012	0.0714	1.65	98.35
22	0.0053	ea. 3H.			
23	0.0820	0.0027	0.0793	3.29	96.71
25	0.3443	0.0085	0.3358	2.47	97.53
27	0.0302	ea. 3H.			
29	0.0116	0.0002	0.0114	1.72	98.28
36	0.1641	0.0037	0.1604	2.25	97.75
38	0.4345	0.0165	0.4180	3.80	96.20
39	0.0322	0.0099	0.0223	30.75	69.25
Hole 380A					
5	0.0429	0.0020	0.0409	4.66	95.34
7	0.1508	0.0050	0.1458	3.32	96.68
8	0.0534	0.0012	0.0522	2.25	97.75
10	0.6205	0.0150	0.6055	2.42	97.58
12	0.2257	0.0134	0.2123	5.94	94.06
14	0.0133	0.0017	0.0166	12.78	87.22
16	0.0082	0.0006	0.0075	7.32	92.68
29	0.0201	0.0026	0.0175	12.94	87.06
22	0.0049	0.0014	0.0035	28.58	71.42
26	0.1766	0.0035	0.1731	1.98	98.02
29	0.0370	0.0086	0.0284	23.24	76.76
33	0.0120	0.0033	0.0087	27.50	12.50
40	0.0079	ea. 3H.			
43	0.0580	0.0019	0.0561	3.28	96.72
48	0.0519	0.0014	0.0505	2.70	97.30
52	0.0759	0.0011	0.0748	1.45	98.55
56	0.0847	0.0015	0.0832	1.77	98.23
60	0.1800	ea. 3H.			
66	0.0348	ea. 3H.			
71	0.0371	ea. 3H.			
Site 381					
9	0.1102	0.0024	0.1078	2.18	97.82
10	0.0046	ea. 3H.			
13	0.2195	0.0071	0.2124	3.23	96.47
14	0.0313	0.0013	0.0300	4.15	95.85
19	0.1066	0.0073	0.0993	6.85	93.15
26	0.0344	0.0020	0.0324	5.81	94.19
31	0.2147	0.0012	0.2135	0.56	99.44

increase, primarily diatoms yielding both amorphous silica and organic matter in individual layers, resulting most probably from lesser accumulations of terrigenous material.

Our detailed lithological study suggests that the upper 300-350 meters of Site 381 conforms in age and composition to the 300 meters of upper terrigenous material at Holes 380/380A.

Deposits in the lower part of Site 381 seem to have accumulated as a result of slope processes. Because discontinuities are probable, if not recognizable in them, we virtually disregarded them in the analysis of physical and mechanical properties.

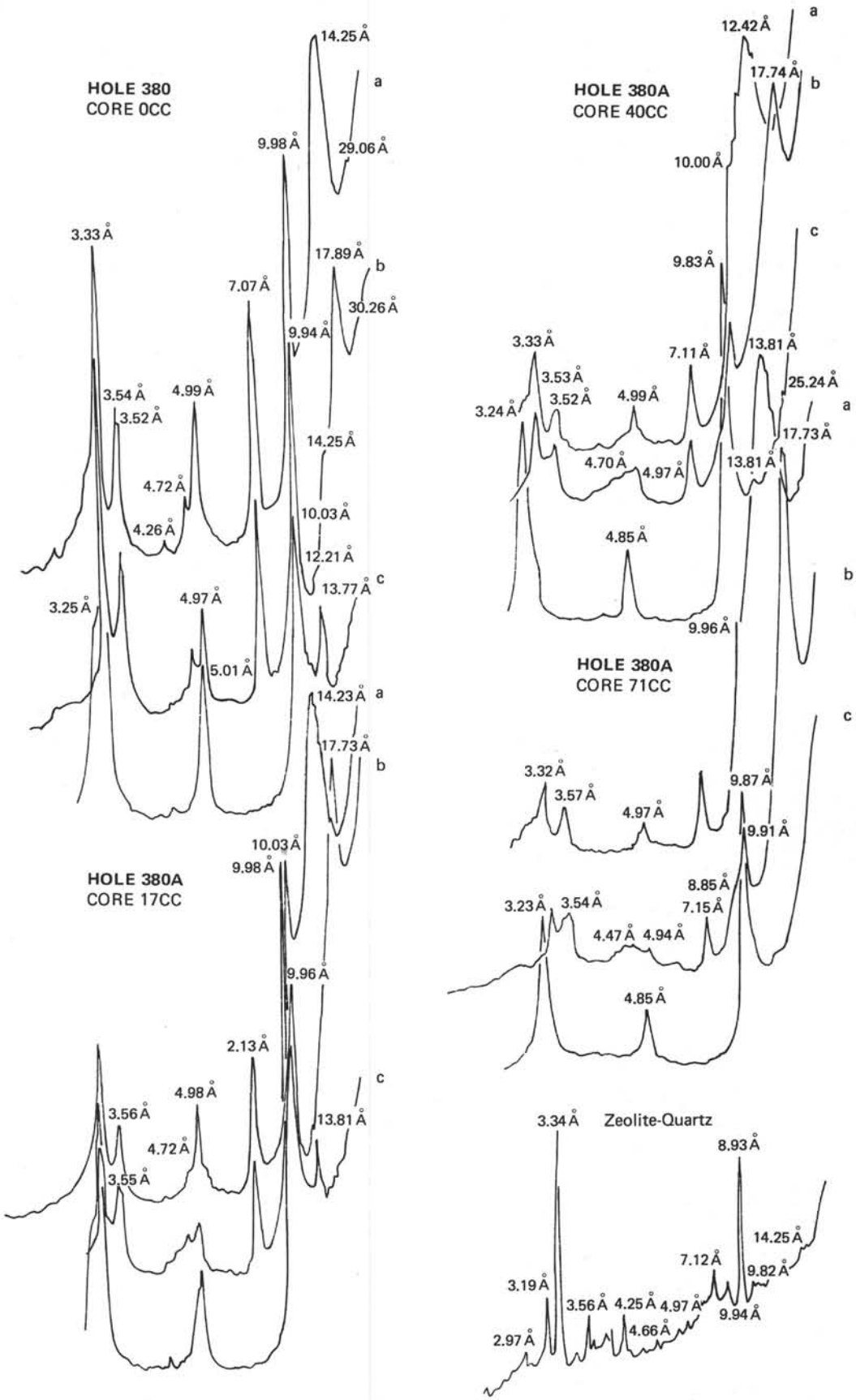

Figure 1. *X-ray diffractograms of the fraction less than 1 μm from sediments at Holes 380/380A. (A) oriented preparation; (B) with glycerine; (C) heated to 550°C.*

TABLE 3
Percentage Composition of Different Clay Minerals (< 1 μm Fraction) From Holes 380/380A and 381

Hole	Core	Composition (%) Clay Minerals, Fraction < 1 =μm				
		Illite	Montmoril-lonite	Mixed-Layer Minerals	Kaolinite	Chlorite
380	0	64	10	10	5	11
380	4	54	10	23	4	9
380	7	55	8	25	5	7
380	9	63	9	13	6	9
380	11	60	12	13	6	9
380	15	50	12	23	7	8
380	17	57	15	15	5	8
380	22	55	12	20	5	8
380	27	60	16	11	6	7
380	33	57	30	–	5	8
380	36	56	16	30	4	4
380	39	48	14	24	6	8
380A	5	51	11	26	5	7
380A	8	42	18	27	9	4
380A	14	53	12	22	7	6
380A	20	51	11	25	6	7
380A	26	46	16	30	3	5
380A	29	38	13	40	6	3
380A	36	42	16	30	8	4
380A	40	36	13	42	4	5
380A	45 mop	52	19	20	5	4
380A	52	46	40	–	9	5
380A	66	52	21	20	4	3
380A	71	30	26	37	5	2
381	7	54	11	22	5	8
381	9	81	9	15	6	9
381	10	42	13	33	9	3
381	13	59	11	16	5	9
381	14	46	33	9	5	7
381	19	49	11	28	4	8
381	22	42	19	30	4	5
381	26	41	19	30	5	5
381	31	40	13	40	4	4
381	33	47	14	30	4	5

PHYSICAL AND MECHANICAL PROPERTIES

Despite attempts at unification (Inderbitzen, 1974; and others), so far there is no unique approach to or strictly elaborated techniques for determination of properties of sedimentary units. It seems appropriate, therefore, to go into some detail and describe the methods we have used.

The granulometric composition of all samples was determined, using the conventional technique based on the particles' settling rate in distilled water. To achieve the complete dispersion of the specimen being prepared for analysis, a wet weighted amount was triturated in 6% sodium pyrophosphate solution. Apart from standard granulometric fractions, the percentage of under 0.22 μ colloid particles was computed. Such ultra-granulometric analysis was carried out for all the 10 samples from Site 381 and for 24 samples from Site 380 and Hole 380A. The results are given in Table 8.

According to the Institute of Oceanology classification, all Site 381 deposits are clay ooze (more than 70% of under 0.01-mm particles). The 0.001-mm fraction accounts for at least 45% and, sometimes 80%. Cores 13 and 33 were exceptions; under the polarizing microscope, these samples contained much carbonate. The maximum dispersity was observed in brownish or brown terrigenous ooze (Core 10), which contained 80.18% of clay particles (under 0.001 mm), and in diatom-sapropel deposits (Cores 22, 26), which contained 63.17% and 66.74% of clay particles. The ultra-granulometric investigation showed an average 50% of Site 381 clay fraction to be colloid particles (under 0.22 μ. The absolute content of colloid particles in these samples varied from 14.53% to 47.03%. The maximum values were observed in high-clay deposits, i.e., colloids increased with rock dispersity. Yet, the relative content of under 0.22 μ particles did not always correlate with the sample's dispersity. For example, a lowered colloid content expressed as percentage of the clay fraction (37% to 48%) was observed in high-dispersed clays with a heightened diatom skeleton content (Cores 22-31), whereas the colloid maximum (64%) was established in a terrigenous ooze sample (Core 14) containing far less under 0.001 mm particles.

From Table 8 it is seen that only four samples (Cores 0, 4, 15, and 36) from Site 380 are silt-clay ooze. The clay fraction in silt-clay deposits varies between 22.39% and 35.76%.

Apart from the investigations described above, a special method of granulometric analysis was used on all samples to assess the structure of the deposits. This was the so-called micro-aggregate analysis, which differs from the standard granulometric method by specimen preparation. A wet-weighted amount was put into a 0.5 l vessel with one-fifth distilled water, and agitated for 2 hours. Subsequent fractionation was carried out as described above. A comparison of the results of granulometric and micro-aggregate analysis provides a notion of the deposits' natural dispersity and aggregation. Aggregation was estimated by $K_{agr.}$ the ratio of a certain fraction's content (as estimated by granulometric analysis) to its content (as estimated by micro-aggregate analysis). Two aggregation ratios were calculated: one for the less than 0.001 mm fraction ($K_{0.001}$) and the other for the less than 0.005 fraction ($K_{0.005}$). The results are shown in Table 9, which shows that practically in all Black Sea deposits, small aggregates less than 0.001 mm in size are present ($K_{0.001} > 1$). Larger aggregates ($K_{0.005} > 1$) are mostly typical of diatom-containing deposits, where they usually reach sand size dimensions. Larger aggregates resistant in a water medium are usually recorded in the lower part of the section: Core 31, Site 381, and especially Cores 40-71, Hole 380A. A higher $K_{0.005}$ is observed in some carbonate-enriched samples (Cores 13 and 33, Site 381; Core 33, Site 380).

PHYSICAL PROPERTIES

We have grouped an important set of data on sediment and rock properties under the general name of "physical properties." These include humidity, plasticity, specific weight, volume weight for various states of the sample, porosity, and sound propagation velocity in various directions (Table 9). Physical properties were studied in samples of disturbed and undisturbed structure.

Humidity

Natural humidity (W_e,%) was estimated as the water mass contained in the sediment or rock relative to the sediment or rock mass dried at 100°-105°C to a constant value (expressed as percentage). The water content in a deposit depends on the granulometric composition, dispersity, mineralogical composition, and organic matter content of the sediment. A high natural humidity, even at great depths, is associated with a high content of clay particles (<0.001), including much montmorillonite and mixed-layer units.

Plasticity

In comparing plasticity limits with natural humidity, a characteristic of the deposit's consistency is obtained. Clay deposits pass from one consistency form into another at certain humidity values, referred to as characteristic humidities or limits.

TABLE 4
Chemical Composition of the Sediments From Holes 380/380A as Determined by X-Ray Fluorescence Analysis

Core	Horizon	Percentage										
		SiO_2	TiO_2	Al_2O_3	Fe_2O_3	MnO	MgO	CaO	K_2O	No_2O	P_2O_5	Lo.i
Hole 380												
5		48.1	0.48	11.95	5.82	0.10	3.15	9.60	2.18	1.29	0.15	17.20
13		49.2	0.68	17.5	6.45	0.06	3.14	5.57	3.18	113	0.12	12.25
15		52.5	0.60	12.4	5.0	0.10	4.05	9.40	2.06	1.29	0.19	12.20
20		48.8	0.66	15.9	7.35	0.08	2.85	7.70	2.89	0.82	0.15	13.10
22		53.0	0.70	15.5	6.14	0.29	3.44	4.94	2.46	1.35	0.10	12.12
23		50.3	0.68	15.3	6.72	0.11	3.61	6.82	2.59	1.28	0.15	12.3
25		50.4	0.68	16.1	7.10	0.11	2.75	6.25	2.73	1.27	0.12	12.5
27		26.8	0.29	8.92	8.38	0.08	2.47	2.40	0.75	1.51	0.07	26.8
29		48.8	2.78	15.1	6.46	0.13	3.28	8.05	2.62	1.25	0.14	13.5
33		49.2	0.63	15.3	6.47	0.15	2.68	7.95	2.57	1.27	0.16	13.6
36	CC	47.8	0.55	12.4	6.60	0.09	2.86	7.88	2.01	1.79	0.20	17.3
38		52.1	0.69	16.6	5.85	0.10	3.30	6.40	3.02	0.95	0.16	10.75
5-4	29-41	55.3	0.66	14.3	5.87	0.10	3.74	4.95	2.31	1.32	0.18	10.4
7-4	85-93	50.5	0.57	12.9	5.05	0.09	4.35	8.15	2.23	1.53	0.15	13.7
Hole 380A												
5		49.2	0.73	17.2	7.46	0.09	2.75	4.43	3.18	2.53	0.11	11.62
7		38.3	0.51	12.4	7.46	0.12	2.91	16.1	1.32	2.27	0.14	17.55
8		49.9	0.65	16.1	7.47	0.04	2.13	5.37	2.56	1.44	0.14	13.8
10		48.7	0.62	14.0	5.94	0.08	2.93	9.95	2.12	1.95	0.13	13.4
12		49.5	0.55	13.5	6.28	0.10	3.40	9.00	2.09	2.41	0.13	13.2
14		27.0	0.26	9.14	7.96	0.12	2.35	24.3	0.41	2.35	0.13	26.2
16		21.4	0.24	8.85	6.78	0.12	2.37	28.7	0.30	2.31	0.09	28.7
18		30.9	0.32	10.5	6.96	0.04	1.95	22.0	0.71	2.45	0.10	24.2
22		20.2	0.20	7.23	9.23	0.12	1.53	29.9	0.53	1.60	0.15	30.1
33		34.4	0.37	11.3	5.80	0.10	2.06	20.5	0.78	2.45	0.15	21.8
36		55.4	0.75	16.8	7.80	0.04	1.87	0.62	2.25	1.88	0.09	11.8
43		53.5	0.40	11.8	4.85	0.05	1.70	6.31	1.28	2.52	0.08	17.6
45		52.2	0.36	10.0	9.25	0.33	1.66	7.20	1.48	2.04	0.17	15.2
48		33.8	0.44	16.8	3.00	0.05	2.38	22.6	0.66	2.37	0.12	23.2
60		24.3	0.26	7.95	4.58	0.11	4.51	26.6	0.60	2.08	0.13	28.9
66		22.5	0.26	7.0	4.50	0.04	7.05	25.6	0.49	2.44	0.08	30.2
75	14-29	51.6	0.79	15.7	6.95	0.07	2.41	3.55	2.55	1.74	0.11	13.9
80	31-47	54.2	0.74	15.4	6.67	0.20	3.27	4.52	2.23	1.94	0.10	11.1

The upper plasticity limit (W_f,%),or the humidity percentage at which the deposit passes from plastic to liquid, was measured using a cup. The lower plasticity limit (W_p,%),or the humidity percentage at which the deposit passes from plastic to solid, was measured by rolling out the specimen to a string until fissures first appeared. The difference of W_f and W_p gave the plasticity number (M_p). Site 380 data show the natural humidity to be above the upper plasticity limit down to a depth of 40 meters, the deposits being in the latent fluid state. At the depth of 250 to 300 meters the natural humidity is a few percent above the lower plasticity limit, falling below it at about 500 meters where the deposits are no longer plastic. For several samples, the hygroscopic humidity (W_h,%) was computed as the difference between total and natural humidity.

From plasticities, the consistency index was computed as

$$B = \frac{W_e - W_p}{M_p}$$

Clay deposits are divided by this value (Table 10).

Specific Weight

Compaction K

$$K = \frac{W_f - W_e}{M_p}$$

was also computed.

The specific gravity (γ,g/cm³) was measured in paraffin oil in a density bottle. Paraffin oil was used to prevent dissolution of salts from the sample which might distort the results. Only data for monolithic samples from Site 381 were obtained (Table 1).

Volume Weight

The wet unit weight of the natural samples (Δ,g/cm³) was measured using 10 cm³ rings. Only monoliths from Site 381 were investigated. For Holes 380/380A, onboard data were used. Compaction and density of the deposits have been found to depend heavily on the composition. For example, the volume weight increase in the 300 to 700 meter interval is

TABLE 5
CO_2 and $C_{organic}$ (Knopp's Method) in Sediments From Holes 380/380A

Core	Horizon	CO_2	C_{org}
Hole 380			
0		7.40	0.47
4	28.5-38.0	5.95	0.62
5-4	29-41	4.14	0.68
5	38.0-47.5	6.75	1.00
7-4	85-93	4.62	1.76
7	57.0-66.5	7.11	1.64
9	76.0-85.5	8.20	0.45
9	76.0-85.5	8.20	0.49
11	95.0-104.9	3.72	1.91
13	114.0-123.0	4.15	0.59
15	133.0-142.5	7.32	0.60
17	152.0-161.0	6.50	0.67
20	180.5-190.0	7.10	0.41
22	199.5-209.5	4.01	0.94
23	209.0-218.5	5.14	0.72
25	–	4.20	0.49
27	247.0-256.5	19.85	0.52
29	266.0-275.5	6.88	0.54
35	304.0-313.5	6.15	0.99
36	323.0-323.5	6.37	2.32
36, CC		4.24	5.23
38		5.61	0.46
39	351.5-361.0	27.72	0.82
Hole 380A			
5	375.0-380	3.20	0.44
7	389.5-399.0	11.25	0.68
7	389.5-399.0	11.15	0.70
8	399.0-408.5	3.70	0.76
10	418.0-427.5	7.00	0.52
12	431.0-446.5	7.19	0.36
14	456.0-475.5	21.07	0.54
16	475.0-484.5	23.00	0.64
18	494.0-503.5	16.90	0.65
20	573.0-522.5	0.52	0.80
22	532.0-541.5	16.51	0.54
26	570.0-579.5	16.00	0.64
29	593.0-598.5	13.47	0.78
33	631.0-636.5	15.30	0.91
36	655.5-665.0	0.20	1.64
40	693.5-703.0	0.17	1.43
43	722.0-731.5	5.90	2.29
45	741.0-750.0	9.50	1.53
48	769.5-779.0	15.30	1.60
52	807.5-817.0	19.58	1.26
56	845.5-855.0	4.25	13.68
60	883.5-893.0	21.40	1.32
66	945.0-950.0	23.35	2.13
CC		16.35	1.88
71	988.6-997.5	3.89	1.74
75	14-29	3.86	1.13
80	47-65	3.21	1.58

linked with a coarser composition and a carbonate enrichment of the deposit. Still, a general increase of the rocks' volume weight with increasing depth is traceable.

From the volume weight of the wet undisturbed sample and from natural humidity, the dry unit weight of the sample (δ,g/cm^2) was computed, or the volume weight of the undisturbed sample whose pores are filled with air. The expression used was

$$\delta = \frac{\Delta}{1 + 0.001\ W_e}$$

TABLE 6
SiO_2 amorphous Content in Sediments From Holes 380/380A

Core	Horizon	SiO_2 amorph
Hole 380		
0		0.80
4	28.5-38.0	1.00
5	38.0-47.5	2.10
7	52.0-66.5	2.00
9	76.0-85.5	0.62
11	95.0-104.9	1.42
13	114.0-123.0	0.92
15	133.0-142.5	0.80
17	152.0-161.0	0.94
20	180.5-190.0	0.84
22	199.0-209.0	1.84
23	209.0-218.5	1.58
25		1.00
27	247.0-256.5	0.70
29	266.0-275.5	0.62
33	304.0-313.5	1.96
36	323.0-323.5	1.16
38		0.56
39	351.5-361.0	0.66
Hole 380A		
5	375.0-380.0	0.90
7	389.5-399.0	1.18
8	399.0-408.5	1.32
10	418.0-427.5	1.00
12	437.0-446.5	1.00
14	456.0-465.5	1.04
16	475.0-484.5	1.06
16		1.04
18	494.0-503.5	1.26
20	513.0-522.5	1.44
22	532.0-541.5	0.80
26	570.0-579.5	0.94
29	593.0-598.5	1.26
33	631.0-636.5	1.14
36	655.5-665.0	4.36
40	693.5-703.0	5.72
43	722.0-731.5	8.30
45	741.0-750.0	9.64
48	769.5-779.0	3.68
52	807.5-817.0	4.68
56	846.5-855.0	3.92
60	883.5-893.0	0.90
66	945.0-950.0	1.16
71	988.6-997.5	1.34
71	988.6-997.5	1.30

Porosity

The porosity (n%) was computed using the expression

$$n = \frac{\gamma - \delta}{\gamma}\ 100\%$$

Only data for Site 381 monoliths were obtained. Porosity was estimated by sample humidity, assuming that all the pores are filled with water. A comparison of porosity values computed by the two methods showed for the sediments concerned (upper part of Site 381) the humidity-based porosity to be much lower than that based on specific and volume weight. This suggests that much of the pore space in the sediments of

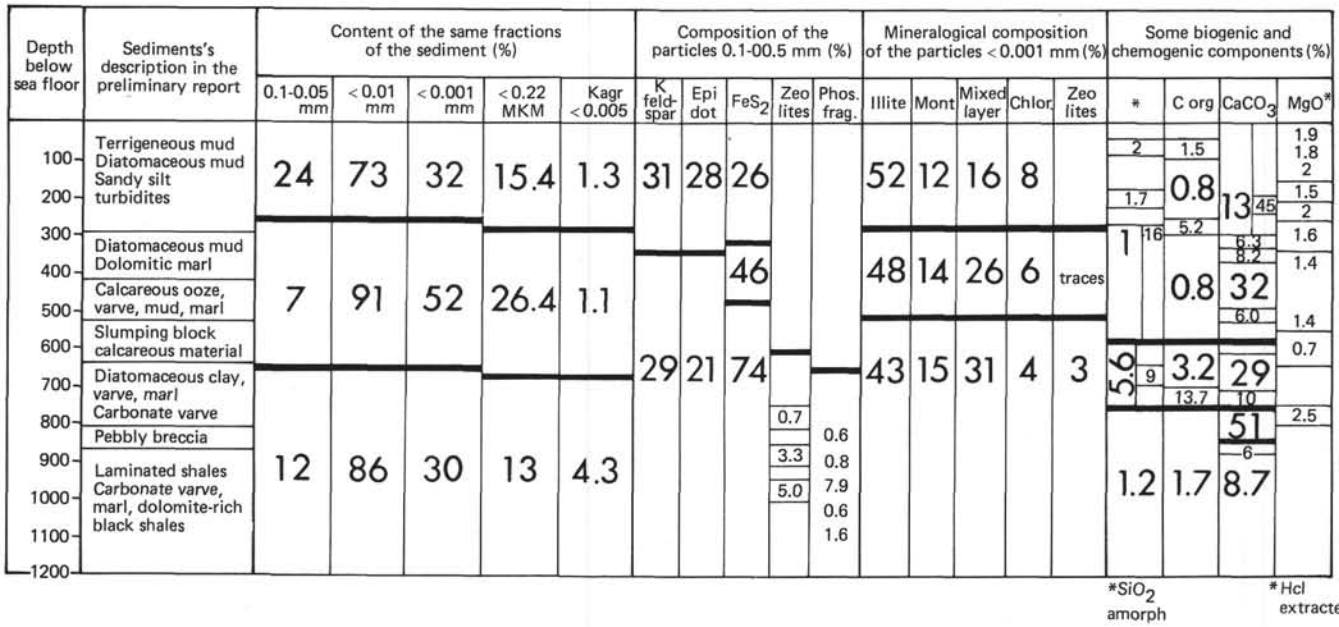

Figure 2. *Changes in the content of some main components of Black Sea sediments. (a) large numbers represent average content of component; (b) small numbers represent maximum content at certain horizons.*

TABLE 7
CaO and MgO (2.5% HCl Extract) Content From Holes 380/380A

Core	CaO	MgO HCl extract
Hole 380		
5	8.40	1.90
13	4.98	1.76
15	7.52	2.17
20	6.40	1.78
22	4.28	1.84
23	5.64	1.96
25	5.20	1.39
27	24.20	1.24
29	6.54	2.05
33	6.84	1.71
38	5.36	1.50
Hole 380A		
5	3.85	1.58
7	14.00	1.88
8	4.82	0.97
10	8.26	1.92
12	8.20	1.90
14	25.45	1.28
16	29.36	1.40
18	22.08	1.05
22	30.44	1.48
33	18.80	1.35
33	18.86	1.34
36	0.60	0.72
43	5.74	0.70
45	6.42	0.79
45	6.38	0.74
48	19.48	0.67
60	26.30	2.52

these horizons is filled with gas. The difference of the two porosities falls to a minimum beginning from the depth of 250 meters (Core 26, Site 381). For older deposits (from Hole 380A), only humidity-based porosity was estimated; for this, skeleton volume weight measured onboard and our natural humidity measurement were used. On the basis of porosity, the index of filtration (ϵ) was computed for Site 381 monoliths.

Sound Velocity

Sound velocity (V_p, m/sec) was measured only in Site 381 monoliths (Table 11); the sound wave propagation was investigated both across (V_p) and along (V_p) the bedding plane. Ultrasonic seismoscopes with frequencies from 50 to 100 kHz were used on samples 10 to 1 cm long. Given the volume weight of wet ground (Δ,g/cm³) and longitudinal wave velocity in it (V_p), we computed the horizon's acoustic stiffness ($\Delta \cdot V_p$) and the index of reflection

$$K_{anz} = \frac{\Delta_2 V_2 - \Delta_1 V_1}{\Delta_2 V_2 + \Delta_1 V_1}$$

We have measured the sound velocity in natural samples artificially compacted with a load of 1.5 kg/cm².

Sound velocity thus grows after compacting the sample. If, before compacting the sample, water is strained through it under the pressure of up to 30 (gradient), the sound velocity grows nearly fourfold against that in the initial natural sample. Compaction without straining raises the sound velocity a mere twofold. Evidently, water strained at a pressure (up to 30 gradient) removes more gaseous phase from the deposit than mere compaction can do. Gas in sediments not only reduces the sound velocity, but brakes their compaction during subsidence.

TABLE 8
Grain-Size Distribution of the Sediments From Holes 380/380A and 381

Core	Type of Analysis	Analytical Data										Calculatal Data			
		> 1mm %	1-0.5 %	0.5-0.25 %	0.25-0.1 %	0.1-0.05 %	0.05-0.01 %	0.01-0.005 %	0.005-0.001 %	< 0.001 %	< 0.22μm μ%	Content of the particles < 0.22μm in the fraction < 1μm	K agreg. for particles < 1μm	< 0.005 mm%	K agreg. for particles < 5μm
Hole 380															
0	granulometrical	–	–	–	1.21	9.59	27.27	9.47	24.63	28.13	10.36	37	1.95	52.76	1.01
	microagregate	–	–	–	1.56	11.62	26.88	7.86	37.68	14.40				52.08	
4	granulometrical	–	–	–	4.13	3.54	28.02	7.92	20.63	35.76	16.10	45	1.94	56.39	1.00
	microagregate	–	–	–	4.65	4.17	28.65	5.18	38.96	18.39				57.35	
7	granulometrical	–	–	–	1.10	1.31	5.58	9.58	32.93	41.37	21.13	51	9.03	14.30	7.78
	microagregate	–	–	–	1.49	3.38	15.65	69.93	4.97	4.58				9.55	
9	granulometrical	–	–	–	0.27	0.58	28.12	10.75	28.39	31.89	14.95	47	4.68	60.28	1.00
	microagregate	–	–	–	–	0.64	22.62	11.79	58.13	6.82				64.65	
11	granulometrical	–	–	–	0.89	1.20	11.79	9.30	29.91	46.91	18.23	39	9.09	76.82	1.54
	microagregate	–	–	–	1.30	4.10	18.26	26.38	44.80	5.16				49.96	
15	granulometrical	–	–	–	3.14	20.88	29.39	9.23	14.97	22.39	12.34	5	5.80	37.36	1.06
	microagregate	–	–	–	2.55	20.43	29.49	12.37	31.30	3.86				35.16	
17	granulometrical	–	–	–	0.45	0.92	22.86	11.35	26.55	37.87	19.77	52	7.65	64.42	1.16
	microagregate	–	–	–	0.93	2.48	25.16	15.92	50.56	4.95				55.51	
22	granulometrical	–	–	–	0.10	0.37	11.95	12.63	33.50	41.45	19.40	47	2.33	74.95	1.78
	microagregate	–	2.07	2.22	6.86	6.94	24.11	15.69	24.35	17.76				42.11	
27	granulometrical	–	–	–	–	0.16	15.32	21.32	33.55	29.65	13.71	46	1.28	63.20	1.09
	microagregate	–	–	–	0.53	1.00	16.36	24.05	34.98	23.08				58.06	
33	granulometrical	–	–	–	0.24	0.33	15.95	11.79	32.02	39.67	18.18	46	6.20	71.69	2.14
	microagregate	2.23	2.23	2.22	4.51	7.96	31.32	16.00	27.13	6.40				33.53	
36	granulometrical	2.06	4.11	6.01	6.50	6.02	27.48	6.90	17.80	23.12	12.02	52	2.04	40.92	1.41
	microagregate	2.29	5.26	6.19	7.22	8.90	32.09	9.11	17.59	11.35				28.94	
39	granulometrical	–	–	–	2.44	0.70	2.63	25.00	48.56	20.67	8.74	42	1.20	69.23	1.14
	microagregate	–	–	–	2.84	0.67	6.52	29.31	43.50	17.16				60.66	
Hole 380A															
5	granulometrical	–	–	–	1.33	0.58	4.49	6.59	36.81	50.20	23.38	47	1.07	87.01	1.01
	microagregate	–	–	–	1.53	0.92	6.32	4.96	39.57	46.70				86.27	
8	granulometrical	–	–	–	7.25	1.80	3.76	1.27	16.52	69.40	43.39	63	1.04	85.92	1.00
	microagregate	–	–	–	10.29	2.00	0.73	1.45	18 69	66.84				85.53	
14	granulometrical	–	–	–	0.71	0.30	5.53	11.60	44.03	37.83	18.54	49	1.12	81.86	1.00
	microagregate	–	–	–	1.20	0.47	2.73	13.08	48.82	33.70				82.52	
20	granulometrical	–	–	–	0.44	0.63	10.37	6.66	30.65	51.25	22.46	44	1.16	81.90	1.04
	microagregate	–	–	–	1.84	1.53	11.37	6.80	34.23	44.23				78.46	
26	granulometrical	–	–	–	0.28	–	15.13	15.28	29.10	40.21	20.87	52	5.55	69.31	1.06
	microagregate	–	–	–	0.56	0.20	17.13	16.97	57.90	7.24				65.14	
29	granulometrical	–	–	–	0.56	0.49	7.52	11.93	35.40	44.10	22.36	51	1.20	78.50	1.00
	microagregate	–	–	–	0.92	0.85	6.37	12.72	42.49	36.65				79.14	
36	granulometrical	–	–	–	0.53	0.65	4.60	1.04	30.73	63.23	32.41	51	1.04	96.96	1.10
	microagregate	–	–	–	2.81	1.42	2.74	4.25	28.20	60.58				88.78	
40	granulometrical	–	–	–	0.33	0.63	4.33	5.83	32.79	56.09	27.86	50	1.45	88.88	1.34
	microagregate	7.61	1.88	1.50	2.35	1.83	6.30	12.06	27.67	38.80				66.47	
45	granulometrical	–	–	–	0.83	0.55	6.45	29.23	29.30	33.64	14.98	45	5.81	62.94	5.09
	microagregate	8.22	1.70	1.23	1.83	1.13	8.97	64.55	6.58	5.79				12.37	
52	granulometrical	–	–	–	1.39	2.72	11.73	15.95	39.29	28.92	13.37	46	5.15	68.21	2.24
	microagregate	12.26	4.67	3.66	6.95	4.10	12.40	25.55	24.79	5.62				30.41	

66	granulometrical	–	–	–	2.67	3.02	6.20	18.25	48.39	21.47	9.42	44	4.91	69.86	7.82
	microagregate	7.22	3.17	2.95	6.68	4.58	15.67	50.82	4.56	4.37				8.93	
71	granulometrical	–	–	–	1.97	3.03	15.73	13.36	29.98	36.93	14.18	38	3.24	65.91	2.65
	microagregate	27.56	4.49	3.12	7.07	6.70	17.17	9.41	13.09	11.39				24.48	
Site 381															
7	granulometrical	–	–	–	0.72	0.89	6.71	3.30	29.14	59.24	27.78	47	7.37	88.38	1.01
	microagregate	–	–	–	1.25	1.04	6.94	3.39	79.34	8.04				87.38	
9	granulometrical	–	–	–	0.73	2.07	6.96	7.39	30.44	52.41	29.57	56	2.86	82.85	1.02
	microagregate	–	–	–	1.09	2.45	8.88	5.39	63.29	18.30				81.59	
10	granulometrical	–	–	–	0.13	–	3.45	2.11	14.13	80.18	47.03	59	18.52	94.31	1.00
	microagregate	–	–	–	–	0.45	2.14	2.73	90.35	4.33				94.68	
13	granulometrical	–	–	–	0.77	1.58	22.58	11.38	34.53	29.18	14.53	50	4.73	69.71	6.40
	microagregate	–	–	–	0.86	2.02	37.66	49.41	3.78	6.17				9.95	
14	granulometrical	–	–	–	0.57	0.44	23.63	8.10	22.62	44.64	28.77	64	4.30	67.26	1.02
	microagregate	–	–	–	1.14	0.46	23.32	8.98	55.71	10.39				66.10	
19	granulometrical	–	–	–	0.71	0.77	7.83	9.61	32.43	48.65	25.96	53	2.55	81.08	1.00
	microagregate	–	–	–	1.39	1.29	8.73	7.07	62.44	19.08				81.52	
22	granulometrical	–	–	–	0.20	0.27	4.29	1.77	26.73	66.74	32.30	48	2.04	93.47	1.05
	microagregate	–	–	–	1.67	1.25	5.94	1.85	56.43	32.76				89.19	
26	granulometrical	–	–	–	0.27	0.56	7.60	3.08	25.32	63.17	29.01	46	2.65	88.49	1.32
	microagregate	–	–	–	10.99	4.15	11.40	6.28	43.30	23.88				67.18	
31	granulometrical	–	–	–	0.54	0.62	3.18	2.92	46.96	45.78	17.12	37	2.63	92.74	1.28
	microagregate	1.64	3.80	4.53	4.70	1.72	5.64	5.57	49.90	22.50				72.40	
33	granulometrical	–	–	–	0.52	1.13	21.20	9.83	38.22	29.10	15.35	53	8.39	67.32	5.33
	microagregate	–	–	–	1.75	1.83	30.34	53.40	9.15	3.47				12.62	

Filterability was measured in more samples than those taken for sound propagation measurement. For two Site 381 monolith samples it was measured experimentally, using a device for investigation of compression properties. A ring holder with the sample, 2 cm high and 25 cm² in section, was placed under a piston, locked in a fixed position. Water was fed into the sample from below. The pressure gradient varied from 0 to 30. The time of the lowering of the water level in the feeder vessel was registered. Standard formulas were then used to compute the filterability (Table 12).

MECHANICAL PROPERTIES

Another major group of sediment and rock qualities comprises data referred to as "mechanical properties." These are indicators characterizing a sample's response to various mechanical actions. The core of this group of properties is made up of various strength indicators (Table 13).

Measured were: compressive strength (δ, kg/cm²), several alternatives of shear strength (τ, kg/cm²), and plastic strength (P_m, kg/cm²).

In addition, the samples were subjected to compression and deformation tests.

The plastic strength (P_m, kg/cm²) was measured using a cone (which had the angle of 45° for loose deposits, and 30° for denser deposits) on the Rebinder plastometer and on the device described by Amelina and Shchukin (1970). It was measured both for the force directed normally and for that parallel to the bedding plane. The ratio of the two values gave the anisotropy coefficient (K_{anis}).

In order to measure the shear strength with the two-plane shear method, parallelepipeds of 1 cm² square cross-section (S) and a length (l) of 2.5-3.0 cm were cut out of the monolithic samples (Site 381). A 1 cm² punch was used to eject a cube from the sample. In this manner, the two-plane shearing was performed. The force applied to the punch was fed through a spring to the recorder, which traced the curve showing the variation of deformation (ΔL) relative to the pressure (P). From these curves (Figure 3), the maximum shear stress (τ_{max}, kg/cm²) and the minimum steady shear stress (τ_{min}, kg/cm²) were computed according to the expression

$$\tau = \frac{P}{2S}.$$

τ_{max} was measured both parallel ($\tau_{max} \parallel$) and normal ($\tau_{max} \perp$) to the bedding plane. The ratio of the two values, $\tau_{max} \perp / \tau_{max} \parallel$, characterizes the deposit's anisotropy. The unconfined compression (σ, kg/cm²) was measured on the same device, but using a different sample shape, i.e., 20-25 cm high and 10-15 cm across. The measurement procedure was the same as above. Compressive stress was computed as

$$\sigma = \frac{P}{S}.$$

The stress which destroyed the sample was taken to be the compressive strength. It too was measured on the force parallel and normal to the bedding plane. From the shear stress and the axial compression, the elastic modulus, E

$$E = \frac{\sigma}{l}$$

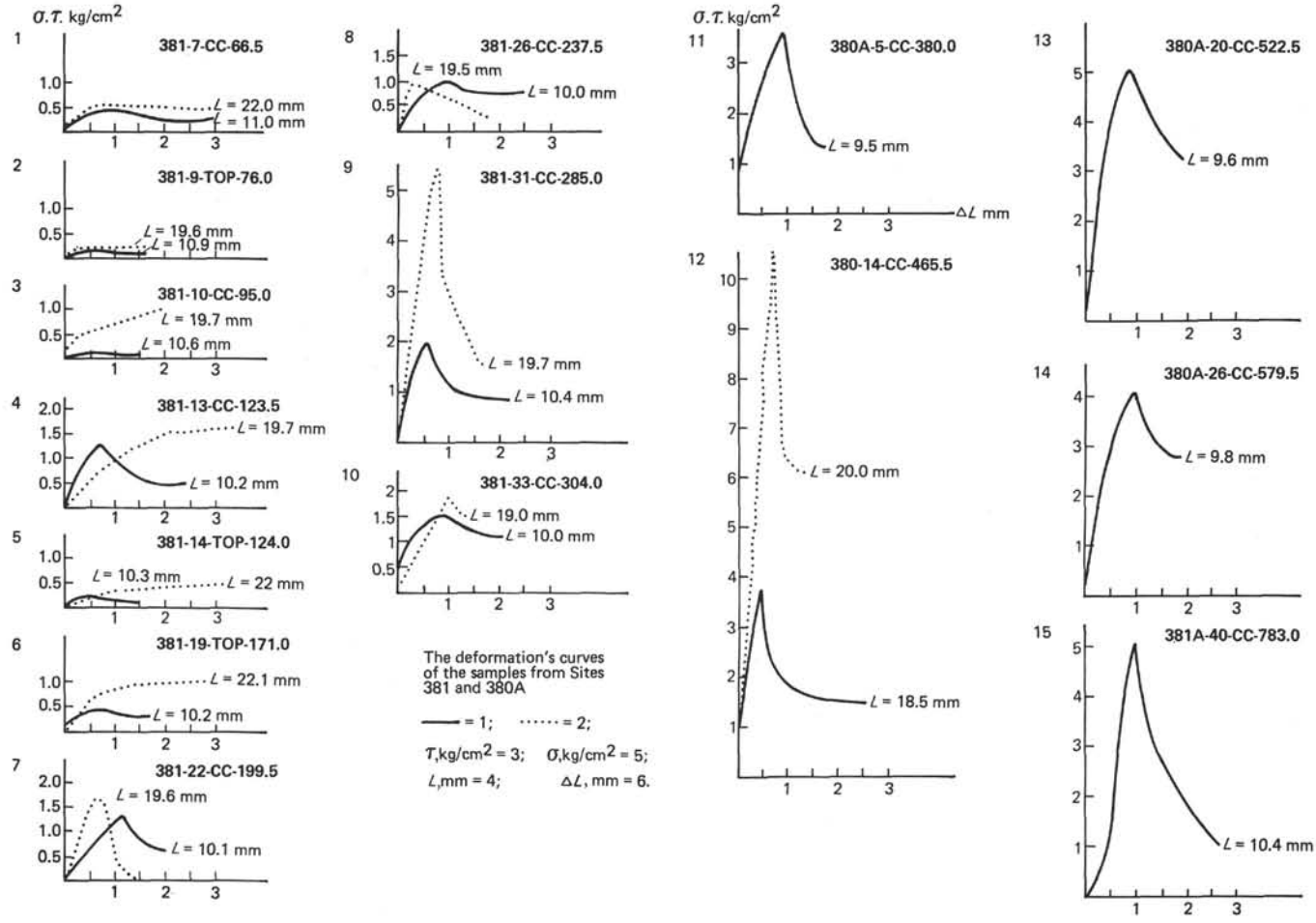

Figure 3. *Shear test information curves of samples from Site 381 and Hole 380A. (1) solid curve showing relation between shear stress and absolute deformation; (2) dotted curve showing relation between compressive stress and absolute deformation; (3) shear stress (τ) in kg/cm^2; (4) length of sample (L) in mm; (5) compressive stress (σ) kg/cm^2; (6) absolute deformation (Δ) in mm.*

was computed, where 1 is the deformation ratio

$$(1 = \frac{\Delta L}{L}).$$

The period preceding the shear was regarded as the process of the sample's elastic deformation under compression.

In attempting to elucidate the nature of the strength properties of the Black Sea deposits under investigation, we employed the data of analyses to evaluate the strength of the individual contact between particles (P_1, dynes). The evaluation was based on the globular model of a dispersed porous body proposed by Shchukin et al. (1970). On this model, the strength of the individual contact between particles is $P_1 = P_c/\chi$ where P_c is the tensile strength estimated as

$$P_c = \frac{\sigma}{G+10}.$$

Here σ is the compressive strength, and the divisor is connected with the sample's plasticity; χ is the number of contacts per cross-section unit, estimated from

$$\chi = \frac{1}{4r^2 \cdot n^2}$$

where r is the radius of the particles, or micro-aggregates, which, by way of convention, are assumed to be spherical, and n is the sample's porosity.

According to the globular module, the individual contact is considered coagulative at $10^{5} < P_1 < 10^{3}$ dynes, condensative at $10^{4} < P_1 < 10^{2}$ and crystallizing at $P_1 > 10^{2}$ dynes.

The investigation of the deformation properties of Site 381 deposits included measuring the volume variation of the sample drying under natural conditions. A ring (h = 2.8 cm, d = 1.5 cm) was used to cut out of the monolith a sample of a given volume V_1. The sample was dried out at room temperature, and its volume, V_2, was measured. The volume shrinkage was computed as

$$\frac{V_1 - V_2}{V_p} \cdot 100.$$

TABLE 9
Physical Properties of Sediments From Holes 380/380A and 381

Core	Horizon	We (%)	Wt (%)	Wp (%)	Mp	Wh (%)	Δ (g/cm^3)	δ (g/cm^3)	δ (g/cm^2)	η% γ · δ	η% δ · We	Kw We/Wn	ε	B	Kd	Vp ⊥ (m/sec)	Vp ∥ (m/sec)	Kan	Cop
Hole 380																			
0	0-95	53.99	40.38	22.15	18.23		1.58							1.75	−0.74				
4	28-38	53.38	52.83	28.39	24.44		1.64							1.02	−0.02				
5	38-47.5	45.91	58.52	29.41	29.11		1.63							0.57	0.43				
7	57-66.5	57.10	71.04	41.48	29.56		1.58							0.53	0.47				
9	76-85.5	38.43	47.66	26.83	20.83		1.71							0.56	0.44				
11	95.0-104.5	43.89	66.41	38.66	27.75									0.19	0.81				
13	114-123	40.49	54.95	29.08	25.87		1.81							0.44	0.56				
15	133-142.5	30.75	34.50	21.69	12.81		1.71							0.71	0.29				
17	152-161	30.44	48.00	26.37	21.63		1.88							0.19	0.81				
20	180.5-190	33.97	47.07	24.76	22.31		1.70							0.41	0.59				
22	199.5-209	39.20	56.88	32.39	24.49		1.70							0.28	0.91				
23	209-218.5	41.63	43.89	27.14	16.75		1.79							0.87	0.13				
25	228-237.5	46.21	52.99	28.84	24.15		1.57							0.72	0.28				
27	247-256.5	28.01	46.03	26.62	19.40		1.83							0.07	0.93				
29	266.0-275	27.04	43.26	31.67	11.59		2.08							−0.40	1.40				
33	304-313.5	26.40	59.95	34.16	25.79		1.76							−0.30	1.30				
36	323-332	38.32	47.96	28.13	19.83		1.93							0.51	0.49				
38	342-351	30.74	37.71	25.11	12.60		2.09							0.45	0.55				
39	351.5-361	44.55	46.77	31.49	15.28		1.92							0.85	0.15				
Hole 380A																			
5	375-380	30.08	54.38	26.54	27.84		1.84							0.13	0.87				0.80
7	389-399	30.38	48.05	26.32	21.73		1.87							0.19	0.81				
8	399-408	47.93	56.41	31.10	25.31		1.95							0.66	0.34				
10	413-423	32.55	42.92	24.41	18.51		1.93							0.45	0.56				
12	437-447	28.13	42.91	25.21	17.70		1.94							0.16	0.84				
14	450-466	31.04	46.53	26.21	20.32		2.01							0.24	0.76				0.54
16	475-485	28.54	44.88	27.80	17.08									0.04	0.96				
18	494-504	28.33	45.05	26.14	18.91		2.02							0.12	0.88				
20	513-522	27.94	56.52	31.15	25.37		2.00							−0.13	1.12				0.87
22	532-542	24.13	48.39	25.63	14.70		2.00							−0.10	1.10				
26	570-580	26.54	50.21	26.70	23.51		1.97							−0.01	1.01				0.63
29	593-599	33.13	55.06	30.83	24.23		1.98							0.09	0.91				
33	631-637	32.51	54.12	32.04	22.08		2.01							0.02	0.98				
36	656-665	38.97	63.94	46.15	22.79		1.84							−0.32	1.32				0.90
40	694-703	50.29	81.12	49.49	31.63		1.79							0.03	0.97				0.87
43	722-732	48.64	70.75	51.61	19.14		1.77							−0.16	1.16				
45	741-754	31.65	79.02	51.52	27.50		1.66							−0.72	1.72				0.77
48	770-779	34.19	54.98	38.06	15.92		1.85							−0.31	1.31				
52	808-817	29.14	51.08	35.16	15.92		1.86							−0.38	1.38				0.78
56	846-855	44.59					1.89												
60	884-893	23.80	36.86	25.17	11.69		2.41							−0.11	1.11				
66	945-950	30.96	41.45	27.57	13.88		2.07							0.68	0.32				
71	988-998	23.55	50.00	33.16	16.84		1.91							−0.57	1.57				0.90
Site 381																			
7	57-66.5	49.46	59.47	34.18	26	5.69	1.61	2.77	1.07	61	53	0.87	1.59	0.53	0.40	570	480	0.84	0.68
9	76-85.5	46.71	55.47	31.87	24	5.26	1.59	2.59	1.08	58	50	0.87	1.40	0.62	0.37	366	358	0.98	0.38
10	855-950	51.57	63.78	37.35	26	7.00	1.49	2.83	0.98	65	51	0.78	1.89	0.55	0.47	342	358	1.05	0.25
13	114-123.5	28.21	44.70	25.90	19	2.21	1.91	2.56	1.49	42	42	1.00	0.92	0.12	0.87	980	1030	1.05	0.57
14	123.5-133	39.47	44.90	24.95	20	3.73	1.70	2.75	1.22	56	48	0.86	1.25	0.73	0.27	420	355	0.85	0.47
19	171-180.5	43.14	55.01	30.75	24	4.21	1.60	2.67	1.12	58	48	0.83	1.38	0.52	0.49	370	300	0.82	0.34
22	195-199.5	54.13	81.65	45.09	59	6.64	1.62	2.69	1.05	61	57	0.93	1.56	0.28	0.71	550	730	1.33	0.56
26	223-237.5	61.39	84.00	43.70	40	6.92	1.60	2.58	0.99	62	61	0.98	1.61	0.44	0.57	560	805	1.44	0.66
31	275-285.0	50.84	70.15	45.12	31	4.03	1.61	2.67	1.03	61	59	0.96	1.59	0.38	0.62	930	1050	1.13	0.67
33	264	41.69	51.25	54.43	17	1.48	1.81	2.60	1.28	51	53	1.00	1.03	0.43	0.56				~0.50
33	304	39.98	54.87	31.71	23	2.51	1.79	2.54	1.28	50	51	1.00	0.98	0.35	0.65				

In that the large volume shrinkage of the Core 22 sample is linked with its peculiar composition, one can say in general that below the depth of 250 meters, the volume shrinkage is small (Table 14).

Rather curious data have been obtained from flocculation experiments on the samples. Two cubic centimeter wet specimens were taken from each sample. The cubes were put on a metal net with 1-cm meshes, the net placed on a support in a vessel and saturated with distilled water. For 17 days, observations were made.

The results of these tests are given in Table 15. The data for Site 381 and Hole 380A are grouped so that they characterize a common section of deposits from the depth of approximately 60 meters sub-bottom down to almost 1000 meters.

The test showed that down to about 300 meters sub-bottom, the sample in distilled water becomes completely distorted.

Above this level, except at about 100 meters, the entire underlying series of deposits are destroyed in distilled water, whereas below it the beds are distorted but not destroyed. Still lower, in the 300-800 meter interval, the water sample interaction produces distortion but not destruction. Samples of rocks from under 800 meters were virtually unaffected by water.

The samples' natural textures were also investigated. By texture we refer to the spatial arrangement (orientation) of structural elements, independent of their size, i.e., unit particles, aggregates, microblocks, etc., of which the sediment or the rock is composed. Both meso- and microtexture were studied.

The mesotexture, or the orientation of the structural elements larger than 1 to 5 μ was examined under the optical microscope. Polished sections were prepared from oriented samples dried at room temperature. Only monolith samples

TABLE 10
Classification of Clay Deposits by Consistency Index

Solid	$B < 0$
Semi-solid	$0 \leqslant B \leqslant 0.25$
Tight-plastic	$0.25 < B \leqslant 0.5$
Soft-plastic	$0.5 < B \leqslant 0.75$
Fluid-plastic	$0.75 < B \leqslant 1$
Fluid	$B > 1$

TABLE 11
Sound Velocity Changes of Two Samples From Site 381 Under Different Compactions and Load

Sample	Sound Velocity in Sample Before Compaction (m/sec)	Sound Velocity After Compaction With a Load of 1.5 kg/cm^2, Without Straining Water Through Sample (m/sec)	Sound Velocity After Straining Water Through Sample and Compacting it Under 1.5 kg/cm^2, (m/sec)
381-9-top	366	620	–
381-19-top	370	–	1320

TABLE 12
Filtration Coefficient of the Same Samples as in Table 11, Under Varying Pressure Gradients

Sample	Coefficient of Filtration (cm/sec) Pressure gradient 30	Coefficient of Filtration (cm/sec) Pressure gradient 0	Initial Pressure Gradient
381-14-top	$0.34 \cdot 10^{-7}$	$0.22 \cdot 10^{-7}$	1
381-19-top	$0.40 \cdot 10^{-7}$	$0.30 \cdot 10^{-7}$	0.5-0.7

from Site 381 were studied. Carbonate-enriched deposits (Cores 13, 14, and 33) had no orientation. All the remaining Site 381 samples had an oriented mesotexture, expressed in simultaneous extinction of the clay mass in crossed nicols. However, the orientations differed. In the samples from Cores 7, 9, 10, and 19, the orientation diverged from the bedding plane more than at 40°-45°. In one of these samples, nearly vertical fissure channels, 0.016-0.03 mm across, were observed. Pyrite globule accumulations were present inside them. At great depths (Cores 22, 26, and 31), clay matter particles are oriented in a plane near to that of bedding.

TABLE 13
Mechanical Properties of the Sediments From Hole 380A and Site 381

Core	Depth Below Sea Floor (m)	Direction of the Measurement	σ Kg/cm^2	E Kg/cm^2	τ_{max} Kg/cm^2	τ_{min} Kg/cm^2	K τ	Pm Kg/cm^2	K Pm	χ (quantity of contacts in cm^2)	P_1 power of the individual contact (dyne)
Hole 381											
7	57.0	⊥	0.65	48	0.44	0.24	0.96	1.24	1.27	$0.15 \cdot 10^9$	$6.5 \cdot 10^{-4}$
	66.5	∥	1.03	37	0.46	0.13		0.98			
9	76.0	⊥	0.22	18	0.17	0.09	0.68	0.72	0.85	$0.63 \cdot 10^8$	$4.7 \cdot 10^{-4}$
	85.5	∥	0.28	18	0.25	0.10		0.85			
10	85.5	⊥	0.37	43	0.12	0.09	0.40	0.90	0.98	$0.73 \cdot 10^9$	$5.4 \cdot 10^{-5}$
	95.0	∥	0.21	42	0.30	0.25		0.92			
13	114.0	⊥	1.43	24	0.98	0.46	2.23	2.75	1.72	$0.21 \cdot 10^8$	$7.0 \cdot 10^{-3}$
	123.5	∥	1.21	29	0.44	0.39		1.60			
14	123.5	⊥	0.30	16	0.18	0.13	0.78	0.50	0.83	$0.21 \cdot 10^8$	$1.4 \cdot 10^{-3}$
	133.0	∥	0.18	10	0.23	0.10		0.60			
19	171.0	⊥	1.06	32	0.48	0.36	1.66	0.98	0.78	$0.36 \cdot 10^8$	$2.7 \cdot 10^{-3}$
	180.5	∥	0.46	32	0.29			1.26			
22	195.0	⊥	1.68	86	1.20	0.53	1.58	3.12	0.94	$0.21 \cdot 10^9$	$1.1 \cdot 10^{-3}$
	199.5	∥	1.56	104	0.76	0.42		3.32			
26	228.0	⊥	0.95	64	1.05	0.81	2.44	1.75	1.17	$0.16 \cdot 10^9$	$0.79 \cdot 10^{-3}$
	237.5	∥	0.86	79	0.43	0.29		1.50			
31	275.0	⊥	5.47	159	2.04	0.90	1.13	6.50	1.81	$0.3 \cdot 10^8$	$2.1 \cdot 10^{-2}$
	285.0	∥	3.42	118	1.80	0.72		3.60			
33 cep.	294.0	⊥	1.90	47	1.21	0.80	1.23			$0.92 \cdot 10^7$	$2.6 \cdot 10^{-2}$
		∥			1.36	0.65					
33 memm.	304.0	⊥									
		∥	1.97	84							
Hole 380A											
5	380.0	⊥			3.65	1.31	5.62				
		∥			0.65	0.50					
14	460.0	⊥	6.75	330	2.16	1.52	0.57			$0.38 \cdot 10^8$	$2.5 \cdot 10^{-2}$
		∥	10.6	170	3.80	0.66					
20	518.0	⊥			5.05	3.32	1.00				
		∥			5.05	2.92					
26	575.0	⊥			4.10	2.78	1.23				
		∥			3.32	1.34					
40	700.0	⊥			5.10	1.00	1.24				$2.4 \cdot 10^{-2}$
		∥			4.12	1.08					

TABLE 14
Volume Shrinkage of Site 381 Samples

Sample	Volume Shrinkage
381-7, CC	29.9
381-9, top	32.2
381-10, CC	33.5
381-13, CC	6.2
381-14, top	25.1
381-19, top	18.1
381-22, CC	31.8
381-31, CC	4.5

The microtexture was investigated by the X-ray techniques and scanning electron microscope. The specimens for the scanning electron microscope were specially prepared to preserve their natural state, according to the procedure described by Osipov (1974). Vacuum sublimation drying was used to preserve the deposit's natural texture. A 16-mm-wide, 5-mm-high specimen of undamaged structure and natural humidity was cut from the monolith. For quick freezing, the specimen was immersed for 15-30 seconds in isopentane, cooled in liquid nitrogen to 150°-160°C. After instant freezing, the specimen was transferred to a refrigerator with a vacuum chamber and dried out. The sublimation drying at −40°-45°C and 10 atm vacuum continued for 24 to 36 hours. A cut perpendicular to the bedding plane was investigated. Displaced fragments and particles were removed from the split surface with adhesive tape applied to it several times. The results are presented on photographs (Figure 4). The photographs, as well as the samples themselves, are oriented perpendicularly to the bedding plane. Regrettably, no quantification of the structure and the texture has been carried out on the photographs. We believe, however, that they provide visual qualitative information on the sizes and interaction of the structural elements—particles, aggregates, and microblocks—on the sizes and distribution in the sample of the pores and microfissures, etc. Although only a few samples were investigated, the photographs indicate an alteration, with depth, of the texture and structure of the Pliocene-Quaternary Black Sea clays. From the 200-300 meter interval on (Site 381, Cores 22 and, especially, 31), the clay particles lie closer together, with the loose large-porous structure becoming increasingly monolithic and compact. The sample taken from the depth of 700 meters (Core 40, Hole 380A) is noteworthy. It is rich in diatom skeletons and amorphous, icicle-shaped or tallow-like cement. The cement fills the interstitial pore space and the microfissures, reinforcing the sample. Its source may have been amorphous silica from dissolved diatom skeletons. The sample's photographs also show a lot of spherical cristobalite particles (Figure 5).

From X-ray study, a quantitative estimate of the samples' microtexture has been obtained. The clay particles' orientation was studied on n X-ray diffractometer with CuαK-α radiation, Uα= 35 kv, Iα = 10 ma. Two samples, prepared as described above, were investigated for a quantitative evaluation of the orientation degree. One sample served to characterize the bedding plane, and the other, the perpendicular section. The surfaces were flattened and polished thoroughly. On the diffraction pattern, the first-order 001 basal reflections of clay minerals and reflections 010 were fixed. From the ratio of the integral intensities (I) of these reflections, the orientation coefficient was determined for each sample as $K_{or} = I_{001}/I_{010}$. From the data for the two samples, the orientation degree of each monolith investigated was determined as

$$C_{or} = \frac{K_{or}\parallel}{K_{or}\parallel + K_{or}\perp}$$

TABLE 15
Flocculation of Samples From Hole 380A and Site 381 in Distillate Water

Sample	Interval (m)	Time and Character of the Flocculating
381-7, CC	66.5	Sample was destroyed absolutely and penetrated through the net in 1 hour 30 minutes
381-9-top	76.5	Sample was destroyed absolutely and penetrated through the net in 2 hours 30 minutes
381-13, CC	123.5	Sample was destroyed after 16 hours but it did not penetrate through the net after 17 days
381-14-top	124.0	Sample was destroyed and penetrated through the net after 1 hour 40 minutes
381-19-top	171.0	Sample was destroyed and penetrated through the net after 2 hours
381-22, CC	199.5	Sample was deformed during 1 hour 40 minutes but did not completely penetrate the net after 17 days
381-26, CC	237.5	Sample was destroyed after 2 hours and penetrated through the net after 12 hours
381-31, CC	285.0	Sample was cracked after 17 days, but was not destroyed and penetrated through the net
380A-5, CC	380.0	Sample penetrated incompletely through the net during 12 hours
380A-12, CC	446.5	Sample was destroyed after 16 hours, but it did not completely penetrate the net after 17 days
380A-14, CC	465.5	Sample was cracked after 16 hours, but it was not deformed and penetrated through the net after 17 days
380A-18, CC	503.5	Sample was destroyed after 16 hours, but it did not penetrate through the net after 17 days
380A-20, CC	522.5	Sample was cracked after 16 hours, but it was not deformed and penetrated through the net after 17 days
380A-26, CC	579.5	Sample was cracked and slightly deformed and did not penetrate through the net after 17 days
380A-36, CC	665.0	Surface of the sample was cracked slightly, but it was not deformed after 17 days
380A-40, CC	703.0	Sample cracked along the plane of the sedimentation after 16 hours, but it was not deformed after 17 days
380A-52, CC	817.0	Surface of the sample was somewhat soaked, but essentially did not change after 17 days
380A-56, CC	855.0	Sample was essentially unchanged after 17 days
380A-71, CC	997.5	Sample was essentially unchanged after 17 days

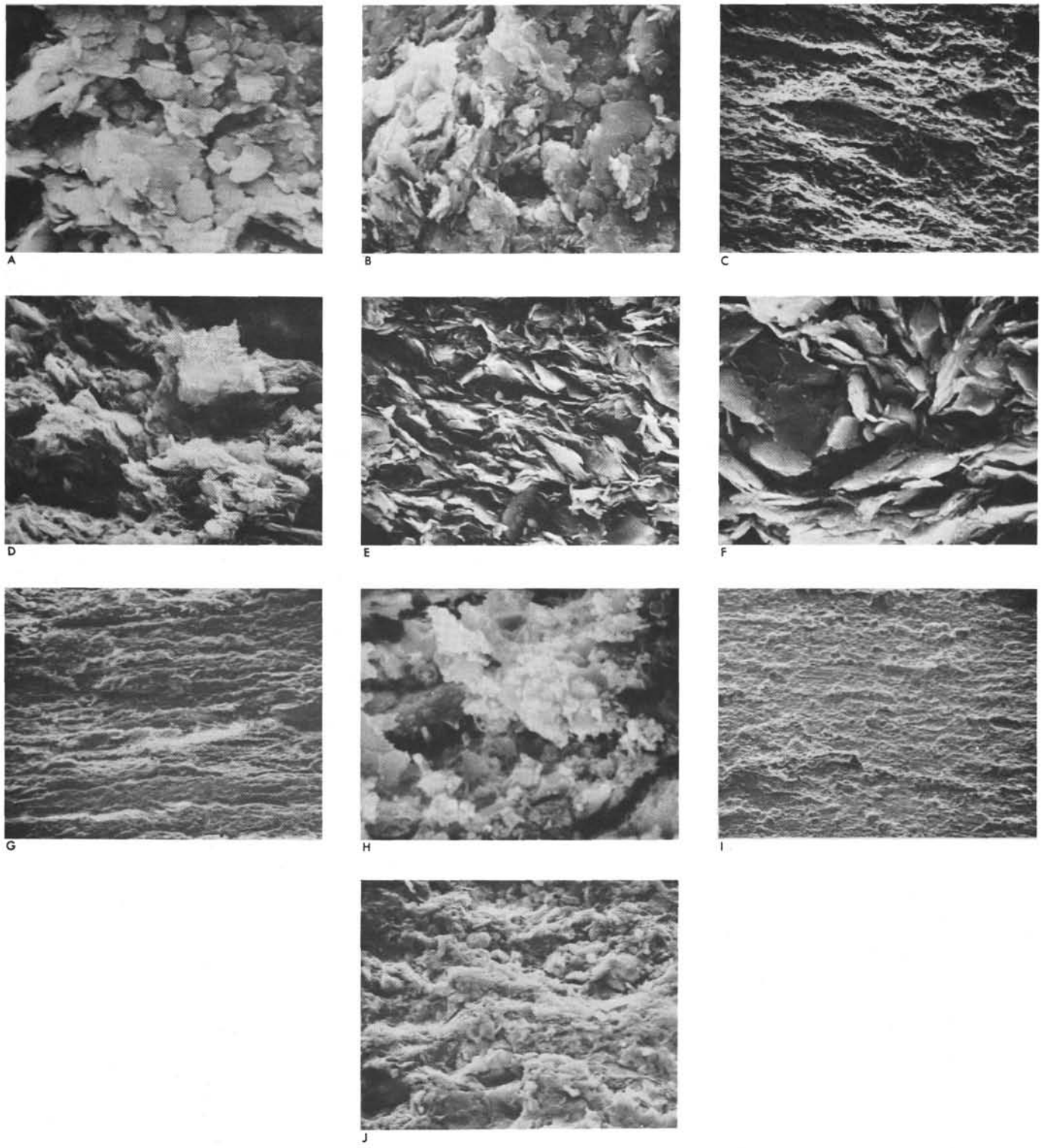

Figure 4. *Photos of samples from Site 381 and Hole 380 with the original (natural) texture after the vacuum dry sublimation. (A) Core 7, CC, Site 381 × 8000. (B) Core 19 top, Site 381 × 5000. (C) Core 22, CC, Site 381 × 5000. (D) Core 22, CC, Site 381 × 5000. (E) Core 5, CC, Site 381 × 5000. (F) Core 5, CC, Hole 380A × 10,000. (G) Core 56, CC, Hole 380A × 200. (H) Core 56, CC, Hole 380A × 10,000. (I) Core 71, CC, Hole 380A × 150. (J) Core 71, CC, Hole 380A × 1500.*

where K_{or} is the orientation coefficient of the sample cut out parallel to the bedding, and $K_{or}1$ is the orientation coefficient of the sample cut out perpendicular to the bedding.

For a maximum orientation of the particles in the plane parallel to the bedding, $C_{or} = 1$, and in that perpendicular to it, $C_{or} \rightarrow 0$. When orientation is random, $C_{or} = 0.5$. In the topspart of Site 381, down to the depth of 200 meters, the orientation degree is mostly less than 0.5, i.e., the clay particles are predominantly oriented in a plane perpendicular to the bedding. Beneath that depth, C_{or} everywhere is more

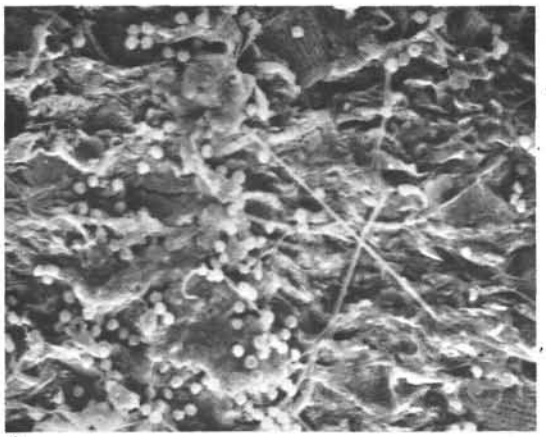

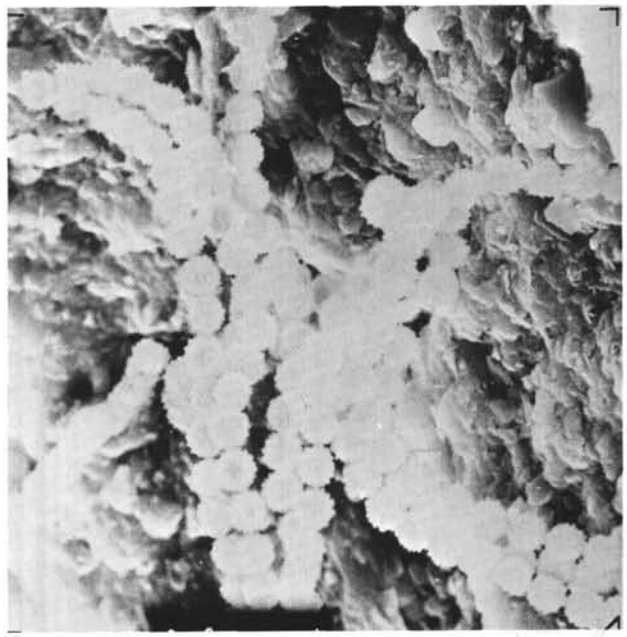

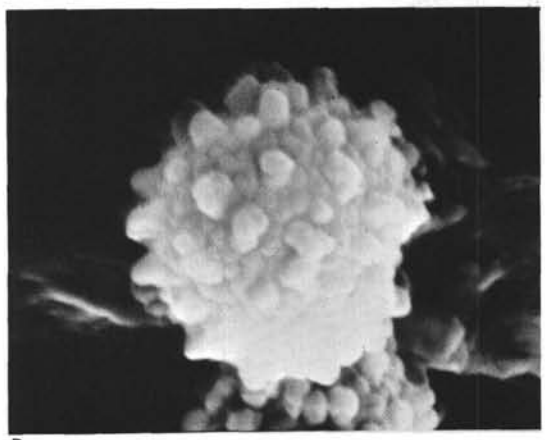

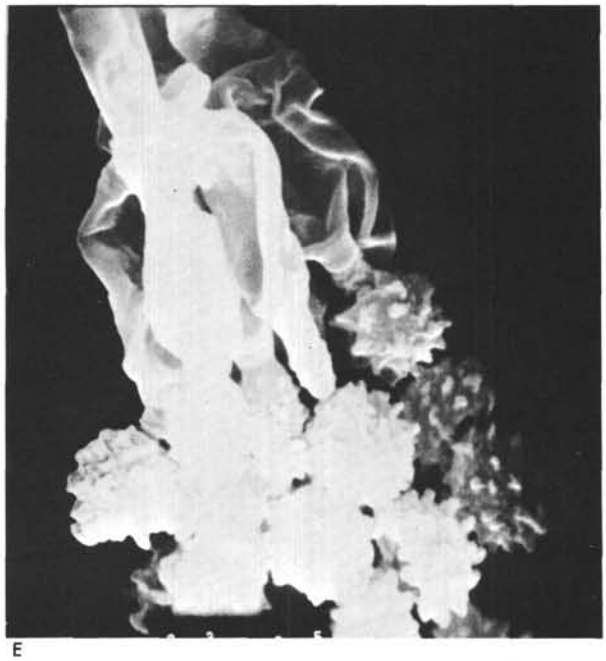

Figure 5. *Cristobalite and SiO_2 amorphous in the samples from Core 40, CC and Core 20, CC, Hole 380A. (A) Core 40, CC × 1000. (B) Core 20, CC × 2000. (C) Core 40, CC × 5000. (D) Core 40, CC × 15,000. (E) Core 20, CC × 7000.*

than 0.5 but not more than 0.67. The further variation of the orientation degree could be tracked for greater depths on samples from Hole 380A which retained their natural structure. The results are given in Table 9. They indicate the orientation at about 400 meters (Site 381, Core 5) to be high, sometimes reaching 0.80. With increasing depth, the clay particles have a tendency for a greater orientation degree in the bedding plane. Against this background of continuous growth, horizons of a lowered orientation occur. The deviations are associated with the lithology of the deposits concerned. In coarser material, clay particles are less oriented. Judging by the lithological description of the sites, the presence of carbonate matter has the same effect. No drop in C_{or} is observed in diatom-containing or amorphous silica-cemented samples.

Scanning electron microscope studies confirm and visualize the growing orientation in the bedding plane of the clay particles with increasing depth, below 199-meter interval (Core 22, Site 381).

DISCUSSION

Having examined all the data obtained on the physical and mechanical properties of the deposits under study, we constructed a composite section for Holes 380/380A and 381. The top part (approximately down to 300 m sub-bottom) of this section is based on specially preserved Site 381 samples, and the lower parts, on Hole 380A. The samples of the section's bottom part proved lithified enough to have retained their natural state.

From the data on the physical and mechanical properties of the deposits features were chosen that visibly varied down the section and clearly illustrated a tendency. These features proved to be the mechanical properties of the deposits, namely the strength indicators, and the rock's soaking degree. Figure 6 presents these parameters.

Figure 6 clearly shows breaks in the physical and mechanical properties which are zones or intervals of various stages of compaction or lithification. The zones or intervals are based on all of the data on the physical and mechanical properties shown in the tables and appendices.

At the top of the section, the zone of most recent deposits, has properties typical of unlithified sediments. It extends down to at least 200 meters sub-bottom. Its main feature is that all the overlying sediments have a shear strength (τ) not more than 1 kg/cm^2. Except for several horizons, the same is true of other strength indicators. The sediments in the upper 200-meter zone also have a high soaking degree. For the most part they are destroyed by water; at least all are strongly distorted. Typically, their humidity always exceeds the upper plasticity limit. Together with a high porosity, this fact correlates with a low orientation degree in the bedding plane observed for the sediment's clay particles. Owing to a high porosity, humidity, and gas content, the upper 200-meter deposits have the lowest sound velocities.

Because we lacked samples from the uppermost horizons, no reliable subdivision of the series into intervals of different lithification degrees was possible. Yet, at least two sub-zones appear to be discernible in the upper 200 meters by physical and mechanical properties, the boundary between them being near the depth of 90 meters. This boundary is indicated by the soaking degree in Figure 6. Indeed, while all sediment samples occurring above 90 meters were fully destroyed by distilled water, several horizons occur below that depth where they are just heavily distorted. A boundary at 90 meters seems to be indicated also by the variation of certain other physical and mechanical indicators, given in tables and appendices.

Beneath 200 meters, an approximately 100-meter-thick transient zone is singled out, apparently comprising a series of deposits where several horizons have rock properties while the others remain essentially unlithified sediments. The zone is clearly indicated in the diagrams of the vertical variation of the characteristics of the deposits' strength, where the zone corresponds to the part of the diagrams occupied by values fluctuating around 1 kg/cm^2.

In the transient zone, other indicators sometimes approach values characteristic of rocks. For example, humidity comes close to the lower plasticity limit, making the deposits highly elastic.

Sharp increase of compression strength, shear strength, etc., occurs at the depth of 300 meters below the sea floor. Even though the compressive and shear strengths in individual horizons vary strongly, the values never fall below 2 kg/cm^2. Other rock properties also undergo a dramatic change. This is conspicuous in the rock texture, where the orientation of clay particles parallel to the bedding is markedly increased. Porosity and humidity are reduced accordingly, which, in turn, raises the velocity of sound waves propagating in the deposit having these properties. The base of the 300-meter-thick series likewise clearly shows, by the soaking degree, that the underlying deposits soaked only slightly; the reaction to distilled water quickly dwindles further down the section. For these reasons, the deposits occurring underneath 300 meters can be considered to be true rock. From this level downward, the variation of all physical properties changes slowly, although that of mechanical properties (strength) continues.

Thus, in the section of the Black Sea deposits under investigation, a zone is distinctly identifiable, in which the deposits are largely unconsolidated, and have not been sediment lithified. The zone embraces a thick interval from 200 to 300 meters beneath the sea floor. It is here that the major change takes place in the sediment. Apparently, the underlying cause is a basic alteration of the spatial arrangement of particles (from random to ordered) and a major strengthening of the structural bonds (strength of individual contact) between them. In the upper 200-meter series, the random distribution of particles leads to a high porosity and humidity. The solid phase-pore water system is largely balanced hydrostatically, weakening the influences of the overlying water column pressure and of the sediment series. With time and continuing deposition of sediment, the particles slowly become oriented and gradually come closer together. Eventually, the pressure of the overlying water and sediment begins to act mostly on the framework of the mass, or its solid particles. As a result, they become oriented parallel to bedding planes, thereby further sharply reducing porosity and humidity. Meanwhile, as the particles come closer to one another, their structural bonds grow stronger (individual contact strength). In all likelihood, these are the processes taking place in the transient zone.

The heightened strength of the rocks beneath 300 meters largely stems from diagenetic processes. First of all, the level

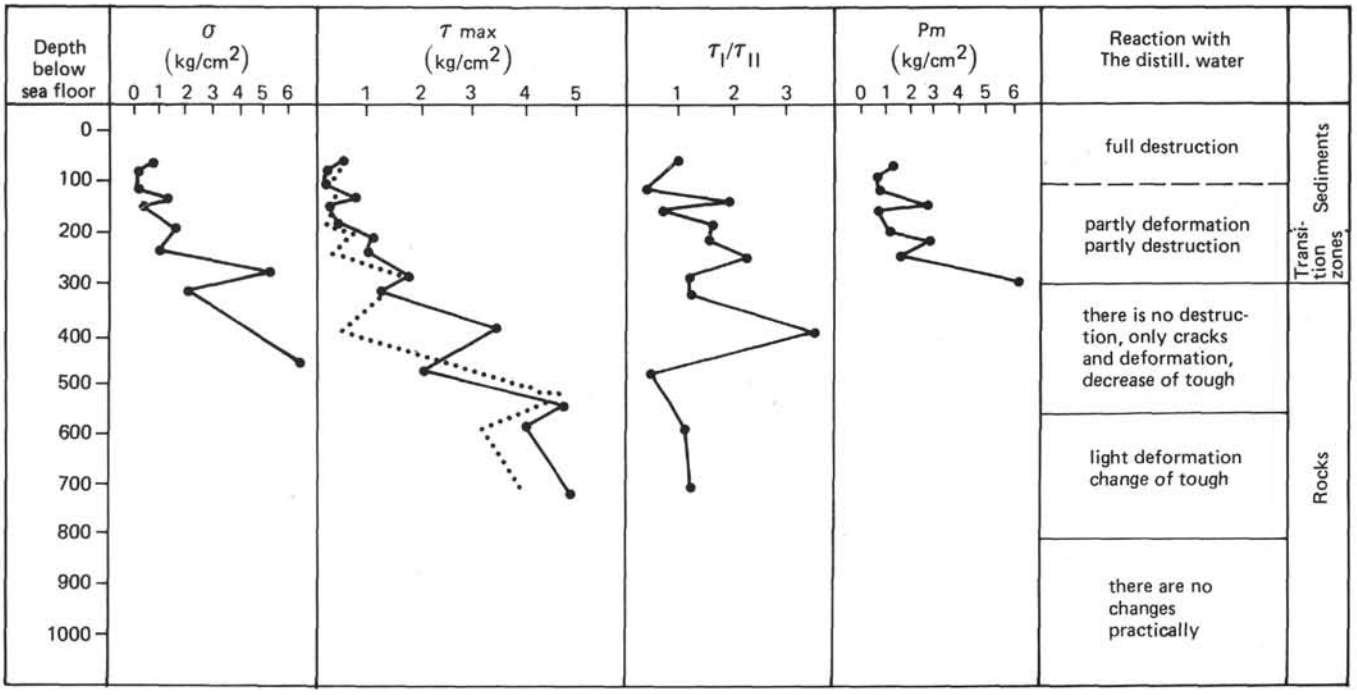

Figure 6. *Changes in the mechanical (deformative) properties of the deposits from Site 381 and Hole 380A and their reaction with the distillate water downsection.*

coincides with a marked increase in carbonate content, a part of the carbonate being obviously recrystallized and functioning as cement. Without this, the lower boundary of the transient zone might well have been somewhat lower than 300 meters. Another cementing element is amorphous silica, or cristobalite, formed from diatom skeletons dissolved in an alkaline medium. This cementing gains in importance below 650-700 meters, giving rise to the irreversible aggregation of colloid and subcolloid particles, the high compressive and shear strength (up to 6 kg/cm^2), and virtually complete loss of capacity for soaking. The latter property warrants referring to the clay rocks at the section's bottom as argillites. Below 700 meters the Black Sea deposits can be considered as a region where intensive catogenetic alteration of rocks begins.

The investigation illustrates a continuous section of the marine sediments' alteration through a transition zone into rocks, in which early and middle stages of catagenesis are recorded.

REFERENCES

Amelina, E. A. and Shchukin, E. D., 1970. Study of regularities of formation of contacts in porous dispersed structures: Kolloid. zhurn., v. 32, no. 6.

Inderbitzen, A. L., 1974. Deep-sea sediments. Physical and mechanical properties: New York (Plenum Press) p. 477-488.

Osipov, V. I., 1974. Preparation of clay specimens for microtexture investigations: Vestnik Moskovskogo universiteta, ser. Geologiya, no. 6.

Shchukin, E. D., Amelina, E. A., Yusupov, R. K., and Rebinder, P. A., 1970. Evaluation of the strength of individual contacts between microcrystals in porous dispersed bodies: DAN SSSR, v. 191, p. 1037.

Weaver, Ch., 1967. Role of clay minerals in sediments. In: Osnovnye aspekty geokhimii nefti: Moscow (Mir Publishers).